Bioorganic & Medicinal Chemistry 25 (2017) 1320–1328

Contents lists available at ScienceDirect

Bioorganic & Medicinal Chemistry

journal homepage: www.elsevier.com/locate/bmc

Studies of TAK1-centered polypharmacology with novel covalent TAK1 inhibitors

Li Tan [a,b,j], Deepak Gurbani [c,j], Ellen L. Weisberg [e,f,j], Douglas S. Jones [g,h,j], Suman Rao [a,b,g], William D. Singer [c,d], Faviola M. Bernard [c,d], Samar Mowafy [a,b,i], Annie Jenney [g], Guangyan Du [a,b], Atsushi Nonami [e,f], James D. Griffin [e,f], Douglas A. Lauffenburger [h], Kenneth D. Westover [c,d,*], Peter K. Sorger [g,*], Nathanael S. Gray [a,b,*]

[a] Department of Cancer Biology, Dana Farber Cancer Institute, Boston, MA 02115, USA
[b] Department of Biological Chemistry and Molecular Pharmacology, Harvard Medical School, Boston, MA 02215, USA
[c] Department of Biochemistry, The University of Texas, Southwestern Medical Center, 5323 Harry Hines Blvd., Dallas, TX 75390, USA
[d] Department of Radiation Oncology, The University of Texas, Southwestern Medical Center, 5323 Harry Hines Blvd., Dallas, TX 75390, USA
[e] Department of Medical Oncology, Dana Farber Cancer Institute, Boston, MA 02115, USA
[f] Department of Medicine, Harvard Medical School, Boston, MA 02215, USA
[g] HMS LINCS Center and Laboratory of Systems Pharmacology, Harvard Medical School, Boston, MA 02215, USA
[h] Department of Biological Engineering, Massachusetts Institute of Technology, Cambridge, MA 02139, USA
[i] Misr International University, Km 28 Cairo, Ismailia Rd., Ahmed Orabi Dist., Cairo, Egypt

ARTICLE INFO

Article history:
Received 23 August 2016
Revised 17 November 2016
Accepted 18 November 2016
Available online 7 December 2016

Keywords:
TAK1
Polypharmacology
Multitarget
Cancer
Cytokine secretion

ABSTRACT

Targeted polypharmacology provides an efficient method of treating diseases such as cancer with complex, multigenic causes provided that compounds with advantageous activity profiles can be discovered. Novel covalent TAK1 inhibitors were validated in cellular contexts for their ability to inhibit the TAK1 kinase and for their polypharmacology. Several inhibitors phenocopied reported TAK1 inhibitor 5Z-7-oxozaenol with comparable efficacy and complementary kinase selectivity profiles. Compound **5** exhibited the greatest potency in RAS-mutated and wild-type RAS cell lines from various cancer types. A biotinylated derivative of **5**, **27**, was used to verify TAK1 binding in cells. The newly described inhibitors constitute useful tools for further development of multi-targeting TAK1-centered inhibitors for cancer and other diseases.

1. Introduction

As summarized in the accompanying article, chemical inhibition of TAK1 has potential utility in treating cancer and inflammatory diseases.[1–5] 5Z-7-oxozeaenol (5Z7) and its analogs are currently the most commonly used probes to chemically interrogate TAK1 kinase activity. 5Z7 forms a covalent bond with Cys174 of TAK1, a residue immediately upstream of the DFG motif (DFG-1), a conserved element in many kinases critical for kinase activation and substrate binding.[6] The most significant off-target effects of 5Z7 and its analogs likely stem from cross-reactivity with other human kinases possessing an analogous cysteine.[6,7] To better understand these activities we profiled 5Z7 at concentrations of 1 and 10 μM against a diverse panel of 456 kinases using an *in vitro* ATP-site competition binding assays (KinomeScan, DiscoverX)[8,9] and found that 5Z7 exhibits a strong inhibition score against many kinases other than TAK1, such as MEKs, PDGFRs and FLTs (Table S1), many of which have a cysteine in the DFG-1 position.

Pharmacological targets of 5Z7 identified by KinomeScan included kinases involved in the TAK1 signaling as well as complementary oncogenic signaling pathways. MEK1/2 (dual serine/threonine and tyrosine kinase), for example, activates downstream effectors in several TAK1-mediated MAPK signaling pathways. Kinases such as TGFBR2 act as direct upstream effectors of TAK1,[10] while ACVR1 (aka. ALK-2) stimulates bone morphogenetic proteins (BMPs) leading to TAK1 activation[11,12] and survival of certain TAK1 dependent cancer cell types.[3] ZAK is another member

DOI of original article: http://dx.doi.org/10.1016/j.bmc.2016.11.035
* Corresponding authors at: Department of Biochemistry, The University of Texas, Southwestern Medical Center, 5323 Harry Hines Blvd., Dallas, TX 75390, USA (K.D. Westover). Department of Cancer Biology, Dana Farber Cancer Institute, Boston, MA 02115, USA (N.S. Gray).
E-mail addresses: Kenneth.Westover@UTSouthwestern.edu (K.D. Westover), Peter_Sorger@hms.harvard.edu (P.K. Sorger), Nathanael_Gray@dfci.harvard.edu (N.S. Gray).
[j] These authors contribute equally.

http://dx.doi.org/10.1016/j.bmc.2016.11.034
0968-0896/

from the MAP kinase family, which also plays key roles in signaling networks overlapping with TAK1.[13] Other pharmacological targets of 5Z7 discovered by KinomeScan analysis are independent of TAK1 signaling and comprise oncogenic signaling cascades such as the RAS-RAF-MAPK pathway and cancer-associated receptor tyrosine kinases (RTK) including PDGFRs, KDR, KIT and FLTs, which activate downstream PI3K/AKT signaling components. Such polypharmacology may support the biological potency of 5Z7.

Despite its evident effects on multiple targets, 5Z7 is often described in the literature as a selective TAK1 inhibitor, and has been widely used in evaluating the therapeutic potential of TAK1 inhibition. There is some evidence that TAK1 is the relevant target for 5Z7 in tumor cells. Proliferation of KRAS-dependent colon cancer cells can be selectively impaired with shRNA knockdown of TAK1, an apparent phenocopy of 5Z7 exposure.[3] Moreover, blocking TAK1 activity with 5Z7 sensitized ovarian cancer cells to cisplatin-induced apoptosis in an analogous fashion to a TAK1 kinase-dead mutant.[2] Inhibition of TAK1 with 5Z7 diminished subarachnoid hemorrhage induced neuronal apoptosis and early brain injury.[14] Upregulation of TAK1 has also been observed in patient-derived acute myeloid leukemia (AML) $CD34^+$ cells, and pharmacological inhibition of TAK1 by 5Z7 correlated with cancer outcomes.[1,15] Nonetheless, given the non-TAK1 inhibitory activity of 5Z7 it is possible that 5Z7-mediated effects are not strictly due to inhibition of TAK1 alone but instead reflect the compound's polypharmacology.

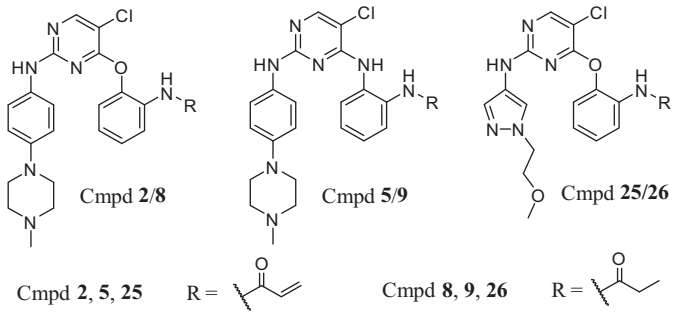

Fig. 1. Exemplary novel covalent TAK1 inhibitors.

To further explore and realize the potential benefits of TAK1-centered polypharmacology, it is necessary to develop potent inhibitors amenable to scale-up and optimization while retaining activity profiles comparable to 5Z7. Such inhibitors will not only assist in evaluating TAK1-centered biology, but will also have potential as leads for further optimization using medicinal chemistry. In our preceding article, structure-guided drug development resulted in discovery of irreversible inhibitors of TAK1 based on a 2,4-disubstituted pyrimidine scaffold. These compounds are capable of covalently reacting with Cys174 in a manner analogous to 5Z7, yet are easily synthesized and accessible for further optimization (Fig. 1). Here we further validate these inhibitors pharmacologically in a number of cancer cell lines and in synovial fibroblasts derived from a rheumatoid arthritis patient.

2. Results and discussion

2.1. Anti-proliferation in Ba/F3 cell lines

Given prior demonstrations of the central importance of TAK1 for KRAS-driven colon cancers, we evaluated the anti-proliferative effects of our inhibitors in KRAS-dependent Ba/F3 cells transformed with oncogenic $KRAS^{G12D}$. Ba/F3 cells are a valuable tool for rapidly evaluating the transforming properties of signal-transduction proteins and for measuring the ability of small molecule inhibitors to inhibit oncogenes. As shown in Table 1, the degree of TAK1 enzymatic inhibition by 25 new and existing small molecules correlated with anti-proliferative activity as measured in $KRAS^{G12D}$ Ba/F3 cells with IC_{50} values in the nanomolar to low micromolar concentration ranges. The majority of the most potent inhibitors were 5-fold less cytotoxic in parental Ba/F3 cells as compared to $KRAS^{G12D}$ Ba/F3 cells demonstrating some degree of selectivity for the transformed state. Several inhibitors were also tested in $NRAS^{G12D}$ Ba/F3 cells with broadly consistent results.

Table 1
Anti-proliferative activities of TAK1 inhibitors against Ba/F3 cells.

ID	TAK1 IC_{50}s (nM)[a]	Ba/F3 cellular IC_{50}s (nM)				
		Parental	$KRAS^{G12D}$	$KRAS^{G12D}$ + IL-3	$NRAS^{G12D}$	$NRAS^{G12D}$ + IL-3
2	5.1	274	28	93	10	61
5	50	7	5	3		
6	83	838	962	763		
7	3.3	234	44	555		
8	>10E4		191	60		
9	1630	8	5	9		
10	25	206	31	376	10	178
11	1640		1352	3732		
12	950	1927	954	1398		
13	92	385	113	357		
14	75	476	57	310		
15	57	1338	181	1192		
16	2750		2012	3530		
17	3010	3274	905		2036	
19	4.4	423	56	745	47	390
20	3.2		74	839		
21	1.7		280	460		
22	7.3	2940	308	859	179	1015
23	7.0	539	67	414	92	277
24	4.6		69	719		
25	2.4	924	154	302		
26	1230	2077	923	3595		
5Z7	5.6		4	12		
AZD			100	>10E4		
BVD		2231	468	8608		

[a] Enzymatic IC_{50}s against TAK1 were obtained with LanthaScreen binding assays.

Compared with their non-covalent counterparts **8** and **26**, the covalent inhibitors **2** and **25** were approximately 6-fold more potent against $KRAS^{G12D}$ Ba/F3 cells. However, **5** and the non-covalent counterpart **9** showed high potency against both parental and transformed lines with EC_{50} values in the single digit nanomolar range despite a biochemical TAK1 IC_{50} value of over 1 μM in the case of **9**. Greater potency on cells than on isolated enzyme is suggestive of substantial off-target activity. Compared to our inhibitors, 5Z7 strongly inhibited the growth of the $KRAS^{G12D}$ Ba/F3 cells without obvious IL-3 rescue suggesting little targeted specificity, while the reported MEK1/2 inhibitor AZD6244 (AZD)[16] or the ERK1/2 inhibitor BVD523 (BVD)[17] exhibited good or moderate potency respectively (Table 1). These results demonstrate that this series of inhibitors is capable of potently inhibiting the proliferation of $KRAS^{G12D}$ Ba/F3 cells but that inhibition of TAK1 is not the sole determinant of this activity.

2.2. Anti-proliferation in cancer cell lines

We analyzed the anti-proliferative effects of the most potent inhibitors in cell lines derived from AML or ALL (acute lymphoblastic leukemia). Cell lines included the mutant KRAS-expressing AML lines, SKM-1 ($KRAS^{K117N}$) and NOMO-1 ($KRAS^{G13D}$); mutant NRAS-expressing AML lines OCI-AML3 ($NRAS^{Q61L}$) and K052 ($NRAS^{G12R}$); ALL lines PF-382 ($NRAS^{G12S}$) and NALM6 ($NRAS^{A146T}$); and wild-type (WT) RAS-expressing AML lines MOLM14, HEL and U937. Surprisingly the FLT3-ITD-dependent line MOLM14 was sensitive to all six covalent inhibitors tested (Figs. 2, S1) and cell growth was fully blocked even at the lowest concentrations tested (31.2 nM) in several cases. However, **2**, **5** and **10**, which possess hydrophilic tails, were more potent than **19**, **23** and **25**, which possess relatively hydrophobic tails. In addition, **25** exhibited better overall potency as compared to its non-covalent counterpart, **26**. With respect to cell line specificity, NALM6 cells were less sensitive to the inhibitors as compared to other KRAS or NRAS mutated lines; the WT RAS cell line HEL was relatively drug resistance whereas U937 was as sensitive as most RAS-mutated lines tested.

Based on these studies, it is not possible to establish a clear correlation between genotype and compound sensitivity. However, **2** and **5** did exhibit good potency against many AML or ALL cancer cell lines and overall potency on liquid tumors was generally consistent with the potency observed against the KRAS-dependent Ba/F3 cells. The exceptional sensitivity of MOLM14 cells to all six inhibitors suggest that covalent compounds also affected FLT3-ITD, which possesses a cysteine residue at the DFG-1 position analogous to Cys174 in TAK1. Indeed we confirmed that compounds **2** and **25** both inhibit FLT3 kinase activity with IC50s of 0.63 and 0.54 nM, respectively.

Next, we examined the anti-proliferative effects of **2**, **5** and **25** and their respective non-covalent counterparts **8**, **9** and **26** in

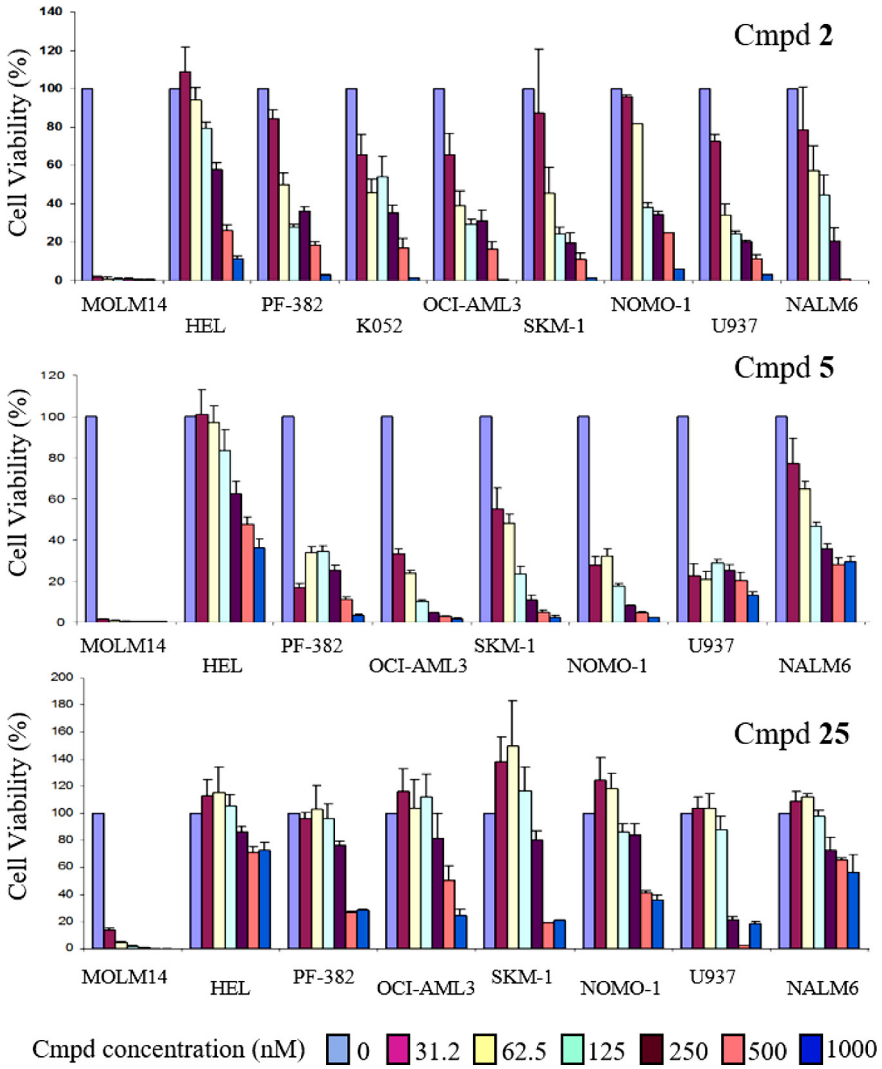

Fig. 2. Percent proliferation of AML or ALL cancer cells challenged by escalating doses of **2**, **5** and **25**.

Table 2
Anti-proliferative activities of TAK1 inhibitors against cancer cells.

ID	Cellular IC_{50}s (nM)					
	Colon		Pancreas		Kidney	
	SW620	SK-CO-1	PANC-1	AsPc-1	SW156	URMC6
2	767	294	1260	1850	2880	524
8	707	213	1360	2700	3730	444
5	67	29	410	18	83	61
9	247	54	426	73	363	263
25	506	318	5610	1340	3020	2620
26	1650	2620	>10E4	5020	>10E4	1490
5Z7	2540	250	2500	6020	2020	1450
AZD	15	117	>10E4	64.2	>10E4	>10E4
BVD	499	356	>10E4	849	1240	>10E4

KRAS-mutated colorectal lines SW620 (G12V) and SK-CO-1 (G12V),[3] pancreatic lines PANC-1 (G12D) and AsPc-1 (G12D)[5] and wild-type KRAS renal cell carcinoma lines SW156[18] and URMC6 (Table 2). Responsiveness to 5Z7, the MEK1/2 inhibitor AZD and the ERK1/2 inhibitor BVD were also evaluated for comparison. Compound **2** showed moderate potency against SW620, SK-CO-1 and URMC6, however, its non-covalent counterpart **8** exhibited similar cytotoxic effects. Compound **5** demonstrated very high potency against all lines except PANC-1, with IC_{50} values ranging from 29 to 83 nM. In addition in most cell lines tested, the anti-proliferative effects of **5** were achieved at 2 to 4-fold lower drug concentrations than those of its counterpart **9**. In contrast **25** was moderately potent against both SW620 and SK-CO-1, however, it showed better potency over its non-covalent counterpart **26**, especially in SK-CO-1 (an 8-fold difference). Surprisingly, 5Z7 was effective (with moderate potency) only in SK-CO-1 cells whereas AZD showed excellent potency against SW620 and AsPc-1 cells, and BVD was less potent than AZD. To summarize, the best inhibitory effects were exhibited by **5** in all six lines tested while **25** exhibited moderate potency against one KRAS-dependent line SK-CO-1.

2.3. Live-cell kinase selectivity

To better understand the spectrum of kinase targets for these inhibitors we profiled **5** and **25** at 1 μM in SK-CO-1 cells utilizing KiNativ technology (ActiveX Biosciences). This live-cell-treatment approach measures binding to potential targets using a competition assay based on a lysine reactive ATP or ADP-biotin probe.[19,20] SK-CO-1 cells were treated with DMSO, 5Z7, **5** or **25** for 4 h, then analyzed as reported previously. Overall 170 kinases were detected in lysates from cells treated with DMSO. Of these kinases, those whose biotin probe-dependent recovery was inhibited by **5Z7**, **5** or **25** are listed in Table 3. MAP3K and MAP2K family kinases were the most strongly inhibited with TAK1 among the top hits. 5Z7 also partially inhibited recovery of RSK1/2/3 and MAP2K6, which all possess a cysteine at the DFG-1 site. Compared to 5Z7, **5** showed 90.5% inhibition of TAK1 with only moderate inhibition of MAP2K1/2 and was weakly active against other potential covalent targets of 5Z7. In addition **5** showed strong inhibition of AURKs and moderate inhibition of MAP3K1, FES and SLK, whereas 5Z7 also inhibited ARAF and HPK1. In conclusion, the overall kinase selectivity of **5** is comparable to but distinct from that of 5Z7. **25** is more selective but, we could not detect binding to TAK1 at 1 μM using the KiNativ assay.

2.4. TAK1 target-engagement

To monitor the degree of TAK1 'target engagement' by **5**, a biotinylated derivative (**27**) was synthesized with a biotin tethered via a flexible PEG linker to the tip of **5**'s tail moiety (Fig. 3A). **27** retained its ability to inhibit TAK1 in a biochemical assay with an IC_{50} at 60 min of 33 nM. We tested two non-small cell lung cancer (NSCLC) lines, H358 or H23, both of which harbor a $KRAS^{G12C}$ mutation and express TAK1 (Fig. S2A). Streptavidin-mediated pull-down of **27** in cell lysates allowed for efficient recovery of TAK1 as assessed by western blotting (Fig. S2B). As expected, **27** did not label TAK1 in the cell lysates following pre-treatment of cells with 1 μM of **5** or 5Z7 (Fig. 3B, C). In contrast, the covalent TAK1 inhibitors **2**, **10**, **20**, **23** or **25** used at 10 μM only partially blocked labeling of TAK1 by **27** and the non-covalent counterparts **8**, **9** or **26** did not have a measurable effect. Unexpectedly, our previously-reported non-covalent TAK1 inhibitor, NG25,[21] inhibited TAK1 in an irreversible manner that was resistant to competition by **27**. This likely reflects the fact that NG25 is a "type-II" kinase inhibitor and therefore has a slow off-rate. This is in contrast with the other TAK1 inhibitors described in this paper that are "type-I" inhibitors, which bind preferentially to the active kinase conformation.

All inhibitors were evaluated in H358 and H23 cell lines for anti-proliferative effects, and compared to inhibitors of MEK1/2

Table 3
KiNativ profiling of **5**, **25** and 5Z7 in SK-CO-1 cells.

Kinases	Inhibition (%)*		
	5	**25**	5Z7
MAP2K1/2	71.7	7.9	95.0
TAK1	**90.3**	31.2	**90.0**
MAP2K1	60.0	-7.9	89.4
ZAK	26.0	-9.2	87.5
MAP2K5	38.1	-59.6	86.8
ARAF	57.0	-15.8	85.5
HPK1	34.9	72.6	77.3
BMPR1A	28.0	19.9	73.1
OSR1	72.9	55.2	72.5
CDK6	51.1	54.5	68.8
FES	77.3	13.6	67.7
RAF1	65.6	6.3	66.4
SLK	76.3	61.2	66.0
RSK1/2/3	42.5	13.0	65.4
PIP5K3	61.5	54.1	64.9
ZAP70	-26.6	34.1	63.6
PLK1	54.6	59.9	61.5
AURKA	87.2	52.6	59.4
AURKB	94.4	65.4	58.1
MLKL	52.3	53.7	56.6
p70S6Kb	3.3	-1.5	54.6
MAP2K6	-43.1	-21.6	54.2
MASTL	49.9	41.3	51.7
MAP3K1	78.5	59.7	51.4

*SK-CO-1 live cells were treated with **5**, **25** or 5Z7 at 1 μM, then lysed labeled with biotin probe, then subjected to mass-spectrometric analysis. Compounds with over 75% inhibition are highlighted with red color, those with over 90% inhibition are highlighted with dark red color.

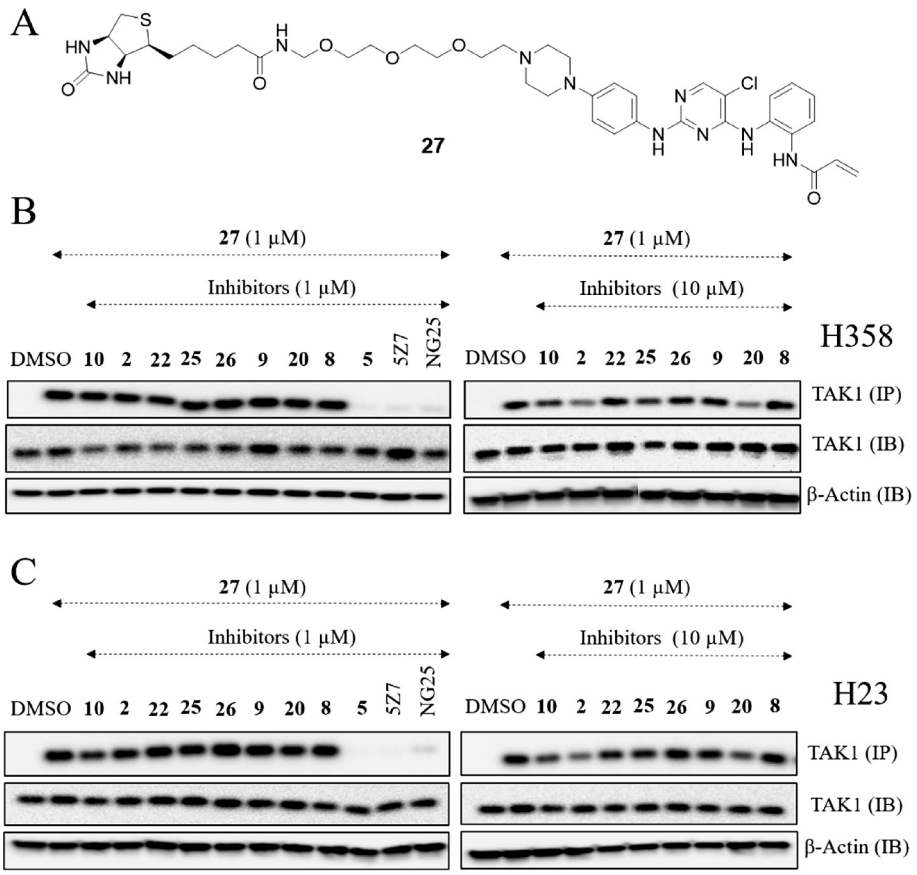

Fig. 3. (A) Chemical structure of **27**. (B, C) Competitive pulldown assay in H358 (B) and H23 (C) cells treated with 1 or 10 μM compounds for 6 h, followed by washout and treatment of the cell lysates with 1 μM of **27** overnight.

(AZD), ERK1/2 (BVD), PI3K (BEZ235), JAK1/2 (Ruxolitinib) and AURKs (VX680) (Fig. S2C). Consistently **2**, **5** and **10** were potent against both lines at very low concentrations; H23, but not H358 cells, exhibited sensitivity to 5Z7, BVD or BEZ235 with IC_{50}s around 1 μM. In contrast, treatment with NG25 or inhibitors of JAK1/2 or AURKs was insufficient to block proliferation at concentrations lower than 5 μM. These results further confirm the cell permeability of our inhibitors, but also suggest that anti-proliferative activities are not a consequence of TAK1 inhibition alone or of inhibition of individual off-target kinases such as AURKs.

We note that some of our biochemically potent covalent TAK1 inhibitors is not as effective as others (e.g. **5**) in labeling TAK1 in living cells. Reasons for this could include conformational difference between recombinant and endogenous native TAK1 proteins, as well as interference from the kinase tracer (Invitrogen[22]) used in the LanthaScreen binding assays. Additionally, unidentified cellular components may interfere. Finally, cellular stability or reactivity with reactive nucleophilic thiol species other than TAK1 could also contribute to decreased potency.

2.5. Proteomic profiling with compound *27*

As another evaluation of kinome selectivity for our covalent TAK1-targeted compounds and to assess non-kinase targets we performed whole-proteome pulldown experiments using the biotinylated probe, **27**, in cell lysates from both H23 and H358 cell lines. Biotinylated proteins recoverable by streptavidin pull down were identified by mass spectrometry. A total of 258 proteins were identified from H23 cell lysate and 255 proteins from H358 cell lysate. Of those, 142 proteins were common to both cell lines (Table S3); 40 proteins were kinases, with 33 commonly identified from both cell lines (Table S4). Some targets such as TAK1, ZAK and MAP2K1 possess a DFG-1 cysteine, consistent with our kinome profiling of compound **5**. However, other kinases lacking the DFG-1 cysteine were also recovered (Table S4). We performed gene enrichment analysis on the list of proteins to determine biological processes, molecular functions and signaling pathways they engage in. Proteins identified were analyzed using the Enrichr software that generated the top 10 hits based on the combined z-score and p-value (Fig. S3B, C, D). In both H23 and H358 cell lines, the proteins pulled down by **27** played a major role in regulating gene expression, followed by initiation of translation and protein targeting to the membrane/ER. The majority of proteins that bound **27**, were ATP-binding proteins with many sharing serine/threonine kinase activities. Another major set of proteins were structural constituents of the 60S/40S subunits of the ribosome and the 28S/39S subunits of the mitochondrial ribosome. Within the subset of proteins commonly inhibited by **27** in H23 and H358 cell lines, signal transduction relating to immune response and the activation of toll-like receptors were the top enriched biological processes. Overall, **27** recovered multiple proteins with ATP-binding properties and serine/threonine kinase activity playing an important role in regulating gene expression, translation, immune-response and Toll-like receptor signaling.

2.6. Inhibition of cytokine secretion

In addition to a role in cancer progression, TAK1 is also implicated in inflammatory disorders.[10] In rheumatoid arthritis (RA), for example, cells that line and maintain the synovium (synovial fibroblasts (SF)) can be activated in culture by cytokines that are implicated in disease progression such as TNFα, IL-1α, and Poly

(I:C). When activated, SF secrete a set of cytokines that are pro-inflammatory, abundant in synovial fluid from RA patients and serve to activate immune cells.[23] The exposure of activated SF to 5Z7 and NG25 normalizes their secretory landscape, in a TAK1dependent fashion.[24] We therefore evaluated the effects of **2**, **5**, **8**, **25**, and **26** to normalize activation of SF from an RA patient (SF donor sample RA2159; Cell Applications, Inc.[24]) using a multi-factorial assay in which Luminex-based sandwich immunoassays were used to profile the levels of 48 cytokines, chemokines, and growth factors. We then computed the effects of inhibitors on cytokines whose secretion was induced using interaction-based multiple linear regression (iMLR; Fig. S4).[24] We then scaled inhibitor iMLR coefficients by the coefficients for TNFα, IL-1α, or Poly(I:C) activators, where 0 indicates no effect and −1 indicates complete inhibition of induced secretion. We found that 5Z7 and **5** were the most potent inhibitors, fully normalizing induced cytokine secretion at a concentration of 0.6 μM (Fig. 4A). NG25, **2**, and **25** also normalized cytokine secretion when used at a higher concentration (3 μM) and the effects of all four inhibitors were significantly correlated (Fig. 4B). The non-covalent counterparts **8** and **26** were virtually inactive at the same concentration. The effects of 5Z7, **2**, **5** and **25** on cytokine secretion by activated SF were significantly correlated, suggesting that similar targets were blocked by all compounds. In contrast, we previously observed that effects of 5Z7 on SF were correlated poorly with the effects of drugs blocking p38, JAK and IKK, other kinases involved in inflammatory signaling in SFs.[24] Taken together these data suggest that despite the structural and polypharmacological diversity of TAK1 inhibitors, they converge to a significantly correlated biological phenotype and that TAK1 is likely the primary functional target of new and existing small molecules.

Multifactorial analysis of activated SF reveals not only beneficial effects of small molecules such as 5Z7 to inhibit inflammatory cytokine secretion, but also potentially counter therapeutic effects. In the case of 5Z7 we observed that it elevated secretion of fibroblast growth factor-basic (FGF-basic; also referred to as FGF-2) in SF that had been activated by TNFα but not IL-1α or Poly(I:C).[24] FGF-basic has been connected to synovial hyperplasia in RA,[25] making its upregulation by a potential RA therapeutic undesirable. We found that **2** and **5**, but not NG25 or **25**, potentiated FGF-basic secretion induced by TNFα (Fig. 4C). The differences between the inhibitors suggest a role for polypharmacology in counter-therapeutic drug activities. Given the favorable specificity profile of **25**, the potentiation of FGF-basic secretion by 5Z7, **2**, or **5** may be

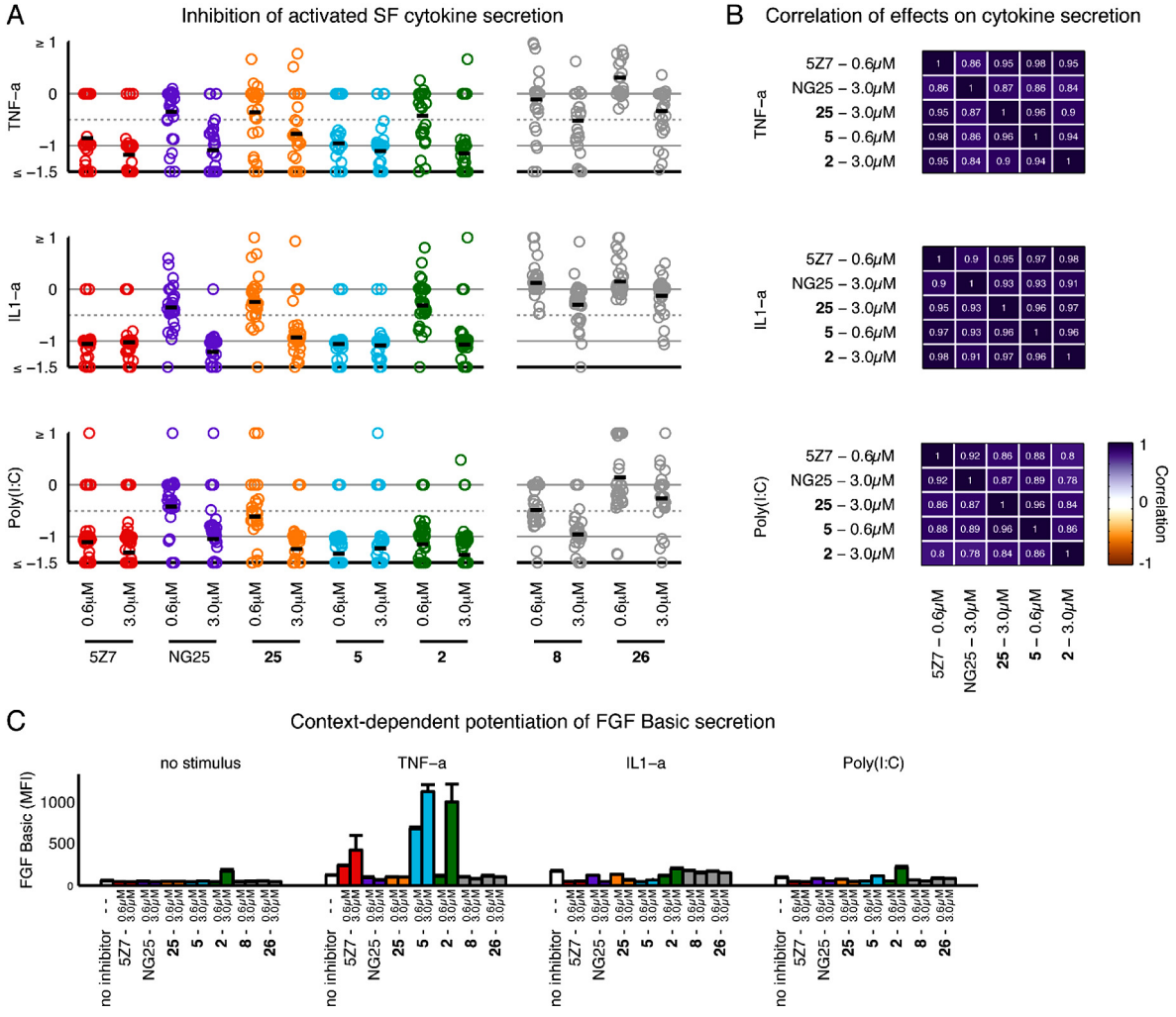

Fig. 4. TAK1 inhibitors block cytokine secretion by activated RA SF. (A) Effect of TAK1 inhibitors on SF activation by TNFα, IL-1α, or Poly(I:C). SF from an RA patient (donor sample RA2159) were pre-incubated with inhibitors (0.6 or 3 μM) or DMSO controls for 3 h prior to stimulation with 10 ng/mL TNFα or IL-1α, or 2 μg/mL Poly(I:C) for 18 h. Supernatants were then recovered and analyzed for secretion of 48 cytokines, chemokines, and growth factors (Bio-Rad 21-plex and 27-plex Luminex cytokine panels). Cytokine secretion data was analyzed by iMLR and inhibitor effects were scaled such that −1 reflects complete inhibition of the secretion induced by the given stimulus. Data points are for individual secreted cytokines. (B) Heat map showing the Spearman correlation matrix of the inhibitor effects across the full cytokine profile. (C) Effect of TAK1 inhibitors on secretion of FGF-basic. MFI: median fluorescent intensity of Luminex beads.

due to an off-target effect rather than TAK1 inhibition per se. Alternatively, TAK1 inhibition might directly potentiate FGF-basic secretion but off-target activities of NG25 and **25** might block this upregulation. In either case, these data demonstrate that not all TAK1 inhibitors have the undesirable property of potentiating FGF-basic secretion and highlight the potential for **25** as a lead molecule for anti-inflammatory therapy.

3. Conclusion

In summary, we evaluated a new series of covalent TAK1 inhibitors in cellular contexts to assess both TAK1-dependent effects and those attributable to polypharmacology. Overall, compound **5** appears to be the most efficient TAK1 inhibitor, and clearly demonstrates covalent binding to TAK1 in living cells as confirmed by pulldown and competitive labeling experiments. Several related inhibitors, such as **2** and **25**, also block TAK1-mediated cytokine secretion in synovial fibroblasts when used at higher concentrations. Many of these inhibitors exhibit good to moderate anti-proliferative effects against RAS-mutated cell lines of diverse cancer types, while **5** stood out for potency and **25** showed favorable overall kinase selectivity. The biotinylated derivative **27** will serve as a useful probe and will help to validate TAK1 inhibition by other inhibitors in living cells. Further investigation of **5** is underway for *in vivo* efficacy and tolerability in RAS-dependent murine tumor models. Meanwhile, the selective inhibitor **25** will be further optimized and evaluated for its therapeutic potential in RA. It should be emphasized that while we present chemical biological evidence that effects observed in these studies are related to TAK1 inhibition, the possibility remains that off-target effects may contribute.

The current study highlights the potential and challenges of kinase inhibitor polypharmacology. In principle, polypharmacology is an undesirable characteristic when developing 'molecularly targeted' compounds for therapeutic purposes.[26] There are, however, theoretical advantages and real life precedents for using 'targeted polypharmacology' to address complex diseases. Indeed, many pathological states such as cancer and diseases of the central nervous system involve multiple genotypic abnormalities, and targeted polypharmacology may provide therapeutic benefits. In oncology the advantage of targeting multiple cellular processes is reflected in firmly established multi-drug regimens used as the current standard of care for treatment of multiple cancer types such as adriamycin, docetaxel, cyclophosphamide and herceptin (ATCH) for breast cancer,[27] adriamycin, bleomycin, vinblastine, dacarbazine (ABVD) for Hodgkin's lymphoma,[28] cisplatin and etoposide (EP) for small cell lung cancer,[29] and vincristine, actinomycin, and cyclophosphamide (VAC) for rhabdomyosarcoma.[30] In an era of molecularly targeted therapies 'combination therapy' has been incorporated into many clinical trials as researchers have gained a more complete understanding of the biological complexities of cancer and have recognized the limitations of targeted monotherapies including the development of drug resistance.[31] Given this background, targeted polypharmacology may have significant advantages not only from a biological perspective, but also from regulatory approval, economic and drug-drug interaction perspectives.[32] Indeed, several agents exhibiting targeted polypharmacology are already used in clinical settings. For example sorafenib is thought to act by a dual mechanism in some contexts with activity against the Ras/Raf pathway inhibiting tumor growth and activity against VEGFR and PDGFR inhibiting angiogenesis.[33,34] Lenvatinib, an inhibitor with activity against VEGFR1-3, PDGFRα, FGFR1-4, RET and c-Kit kinases has also shown efficacy attributable to its multi-target mechanism.[35] The compounds described in this study overlap with 5Z7 with respect to TAK1 inhibition but appear to differ with respect to other targets; thus, they complement 5Z7 and provide valuable tools for studying TAK1-centered polypharmacology in cancer and RA. They may also assist in the identification of novel therapeutic targets whose inhibition would be complementary or synergistic with inhibition of TAK1.

4. Experimental

*4.1. N-(2-(2-(2-(2-(4-(4-((4-((2-Acrylamidophenyl)amino)-5-chloropyrimidin-2-yl)amino)phenyl)piperazin-1-yl)ethoxy)ethoxy)ethoxy)ethyl)-5-((3aS,4S,6aR)-2-oxohexahydro-1H-thieno[3,4-d]imidazol-4-yl)pentanamide (**27**)*

Compound **27** was synthesized with similar procedures as the syntheses of other analogs [REF]. ^{1}H NMR (600 MHz, DMSO-d_6) δ 10.18 (s, 1H), 9.56 (br, 1H), 9.20 (br, 1H), 8.58 (s, 1H), 8.10 (s, 1H), 7.83 (t, J = 5.6 Hz, 1H), 7.76 (d, J = 7.9 Hz, 1H), 7.48 (d, J = 7.6 Hz, 1H), 7.43 (d, J = 8.5 Hz, 1H), 7.34 (m, 1H), 7.27 (m, 1H), 6.81 (d, J = 9.2 Hz, 1H), 6.52 (dd, J = 16.8, 10.1 Hz, 1H), 6.38 (m, 2H), 6.34 (d, J = 17.3 Hz, 1H), 5.81 (d, J = 10.6 Hz, 1H), 4.30 (dd, J = 7.6, 4.6 Hz, 2H), 4.12 (dd, J = 7.8, 4.4 Hz, 2H), 3.80 (m, 4H), 3.57 (m, 4H), 3.41 (m, 6H), 3.21 (m, 5H), 3.08 (m, 2H), 2.94 (t, J = 11.6 Hz, 2H), 2.81 (dd, J = 12.5, 5.2 Hz, 1H), 2.58 (d, J = 12.5 Hz, 1H), 2.07 (t, J = 7.3 Hz, 2H), 1.60 (m, 1H), 1.47 (m, 3H), 1.29 (m, 2H).. MS (ESI) m/z 851 $(M+H)^+$.

4.2. Cell proliferation assays

Tissue culture was performed in a 37 °C incubator containing 5% CO_2. Cells were initially seeded at a density of 1000 viable cells per well of white 96-well plates in 50 μl of tissue culture medium, in the absence or presence of IL-3. Four hours later, nine serial four-fold dilutions of indicated compounds in 50 μl of medium were added to triplicate wells to span a final concentration range of 0.5–30,000 nM. Medium contained 0.3% (v/v) DMSO, and a triplicate of Ref. wells treated with DMSO alone served as 100% viability controls for each experiment. Seventy-two hours after addition of compound, cell viability was determined by addition of CellTiter-Glo reagent (Promega) and determination of resultant luminescence using a Synergy NEO plate reader (BioTek). From resultant plots (GraphPad Prism), IC_{50} values were obtained by nonlinear fit analysis of log (inhibitor) vs. response (three parameters). The $KRAS^{G12D}$ and $NRAS^{G12D}$ transformed Ba/F3 cells were generated as previously described.[36]

H23 and H358 cells were seeded into 384-well plates at a density of 2000 cells/well using the Multidrop Combi Reagent Dispenser (Thermo Fisher) and incubated for 48 h prior to drug treatment. Cells were then treated with varying doses of drugs using the D300 Digital Dispenser (Hewlett-Packard) and incubated for 72 h. Cell viability was determined using 25 μL/well of CellTiter-Glo reagent (Promega) and the luminescence detected using the Synergy H1 Plate Reader (BioTek Instruments Inc.). Dose-response curves and IC_{50} of growth inhibition were calculated using GraphPad Prism 6.0.

4.3. Immunoprecipitation and immunoblotting analysis

H358 and H23 cells were treated with 1 or 10 μM of drugs and incubated for 6 h. Drug containing media was removed, cells were rinsed with cold PBS twice and lysed using the MPER lysis buffer (Thermo Fisher #78501). The resulting lysates were treated with **27** (1 μM) overnight at 4 °C, pulled down with streptavidin beads and analyzed with immunoblotting using the TAK1 antibody from Cell Signaling Technologies (#4505).

4.4. Proteomic profiling of **27**

H23 and H358 cells were grown in 10 cm dishes, extracted and lysed. The resulting lysates were incubated with 1 μM of **27** or DMSO overnight at 4 °C, and pulled down with streptavidin beads. The samples were then run on precast polyacrylamide gels (BioRad), stained with coomassie blue (Thermo Fisher, LC6060) and bands corresponding to pulled down proteins were isolated, digested and analyzed using mass spectrometry. Label-free quantification values (top 3 TIC) were converted from spectral counts using Scaffold 4.7.2 (Proteome Software Inc.) and used to identify proteins pulled down exclusively in **27** treated samples but not DMSO treated. Enrichr[37,38] was used to determine the GO biological processes and molecular functions regulated by the proteins. Pathway analysis was carried out using the KEGG database on Enrichr. Venn diagrams comparing the list of proteins pulled down in each cell line were generated using Venny 2.0.[39]

4.5. Cytokine secretion assays

Cytokine secretion profiles from activated SF were analyzed as described previously.[24] Briefly, primary human RA SF (Cell Applications Inc., HFLS–RA, cat. No. 408RA–05a, lot No. RA2159) were seeded at a density of 1000 viable cells/well into 384-well plates. Following ~24 h in full growth medium (Synoviocyte Growth Medium, Cell Applications, Inc. cat. No. 415–500) at 37 °C and 5% CO_2 cells were starved in basal medium (Synoviocyte Basal Medium, Cell Applications, Inc. cat. No. 414–500) overnight followed by an additional starvation step in basal medium containing 0.1% bovine serum albumin (BSA) around 4 h prior to incubation with stimulatory factors. SF were pre-incubated with inhibitors (0.6 or 3 μM) or DMSO controls for 3 h prior to stimulation with 10 ng/mL TNFα or IL-1α, or 2 μg/mL Poly(I:C) for 18 h. Supernatants from two adjacent wells (e.g. well A1 and A2, which comprised biological replicates) were pooled for subsequent analysis by Luminex cytokine profiling. Downstream statistical analyses considered data from pooled supernatants as a single replicate. Following pooling of adjacent wells. stimulus and inhibitor combination treatments were present in biological duplicate (e.g. biological quadruplicate replicates were pooled to yield biological duplicates), inhibitor in the absence of stimulus was present in biological triplicate, stimulus in the absence of inhibitor was present in biological quadruplicate, and unstimulated controls were present in six biological replicates. Pooled supernatants were adjusted to 0.25% BSA and stored at -80 °C.

Cytokines were measured using a multiplex ELISA-type assay on a Flexmap 3D (Luminex Corp.), using 27-plex and 21-plex cytokines kits (Bio-Rad cat. No. M500KCAF0Y and MF0005KMII). Supernatants were diluted 1:3 with 1xPBS, 0.05% BSA, 0.05% Tween-20 and assayed according to the supplier's instructions. Spiked ligand controls were also included to control for cross-reactivity of the stimulating cytokines against the Luminex reagents (i.e. 10 ng/mL TNFα or IL-1α, or 2 μg/mL Poly(I:C) in basal medium with 0.25% BSA were diluted 1:3 into 1xPBS, 0.05% BSA, 0.05% Tween–20 and analyzed for cross-reactivity against the Luminex components). To control for the background value associated with each cytokine assay, multiple replicates of Luminex beads incubated with "mock" supernatant samples (basal media with 0.25% BSA diluted 1:3 with 1xPBS, 0.05% BSA, 0.05% Tween-20) were also included on each Luminex assay plate and were processed in an identical manner to the experimental samples. Cytokine secretion data was modeled using iMLR as described previously and statistical significance was assessed using a multimodeling framework.[24] β coefficients were taken as significant if at least 50% of the multimodeling frameworks assigned a significant effect for the given coefficient.

Acknowledgements

NSG and PKS were supported by LINCS Grant U54-HL127365. KDW was supported by CPRIT R1207 and CPRIT RP140233. LT and NSG were supported by NIH CA 154303-05 and the Pediatric Low Grade Astrocytoma (PLGA) foundation.

A. Supplementary data

Supplementary data associated with this article can be found, in the online version, at http://dx.doi.org/10.1016/j.bmc.2016.11.034.

References

1. Buglio D, Palakurthi S, Byth K, et al. Essential role of TAK1 in regulating mantle cell lymphoma survival. *Blood*. 2012;120:347–355.
2. Cai PC, Shi L, Liu VW, et al. Elevated TAK1 augments tumor growth and metastatic capacities of ovarian cancer cells through activation of NF-kappaB signaling. *Oncotarget*. 2014;5:7549–7562.
3. Singh A, Sweeney MF, Yu M, et al. TAK1 inhibition promotes apoptosis in KRAS-dependent colon cancers. *Cell*. 2012;148:639–650.
4. Fan Y, Cheng J, Vasudevan SA, et al. TAK1 inhibitor 5Z-7-oxozeaenol sensitizes neuroblastoma to chemotherapy. *Apoptosis*. 2013;18:1224–1234.
5. Melisi D, Xia Q, Paradiso G, et al. Modulation of pancreatic cancer chemoresistance by inhibition of TAK1. *J Natl Cancer Inst*. 2011;103:1190–1204.
6. Wu J, Powell F, Larsen NA, et al. Mechanism and in vitro pharmacology of TAK1 inhibition by (5Z)-7-Oxozeaenol. *ACS Chem Biol*. 2013;8:643–650.
7. Schirmer A, Kennedy J, Murli S, Reid R, Santi DV. Targeted covalent inactivation of protein kinases by resorcylic acid lactone polyketides. *Proc Natl Acad Sci USA*. 2006;103:4234–4239.
8. Goldstein DM, Gray NS, Zarrinkar PP. High-throughput kinase profiling as a platform for drug discovery. *Nat Rev Drug Discovery*. 2008;7:391–397.
9. Miduturu CV, Deng X, Kwiatkowski N, et al. High-throughput kinase profiling: a more efficient approach toward the discovery of new kinase inhibitors. *Chem Biol*. 2011;18:868–879.
10. Sakurai H. Targeting of TAK1 in inflammatory disorders and cancer. *Trends Pharmacol Sci*. 2012;33:522–530.
11. Shore EM, Xu M, Feldman GJ, et al. A recurrent mutation in the BMP type I receptor ACVR1 causes inherited and sporadic fibrodysplasia ossificans progressiva. *Nat Genet*. 2006;38:525–527.
12. Miyazono K, Kamiya Y, Morikawa M. Bone morphogenetic protein receptors and signal transduction. *J Biochem*. 2010;147:35–51.
13. Cho YY, Bode AM, Mizuno H, Choi BY, Choi HS, Dong Z. A novel role for mixed-lineage kinase-like mitogen-activated protein triple kinase alpha in neoplastic cell transformation and tumor development. *Cancer Res*. 2004;64:3855–3864.
14. Zhang D, Yan H, Li H, et al. TGFbeta-activated kinase 1 (TAK1) inhibition by 5Z-7-oxozeaenol attenuates early brain injury after experimental subarachnoid hemorrhage. *J Biol Chem*. 2015;290:19900–19909.
15. Bosman MC, Schepers H, Jaques J, et al. The TAK1-NF-kappaB axis as therapeutic target for AML. *Blood*. 2014;124:3130–3140.
16. Yeh TC, Marsh V, Bernat BA, et al. Biological characterization of ARRY-142886 (AZD6244), a potent, highly selective mitogen-activated protein kinase kinase 1/2 inhibitor. *Clin Cancer Res*. 2007;13:1576–1583.
17. Ward RA, Colclough N, Challinor M, et al. Structure-guided design of highly selective and potent covalent inhibitors of ERK1/2. *J Med Chem*. 2015;58:4790–4801.
18. Fogh J. Cultivation, characterization, and identification of human tumor cells with emphasis on kidney, testis, and bladder tumors. *Natl Cancer Inst Monogr*. 1978;5–9.
19. Patricelli MP, Szardenings AK, Liyanage M, et al. Functional interrogation of the kinome using nucleotide acyl phosphates. *Biochemistry*. 2007;46:350–358.
20. Patricelli MP, Nomanbhoy TK, Wu J, et al. In situ kinase profiling reveals functionally relevant properties of native kinases. *Chem Biol*. 2011;18:699–710.
21. Tan L, Nomanbhoy T, Gurbani D, et al. Discovery of type II inhibitors of TGFbeta-activated kinase 1 [TAK1] and mitogen-activated protein kinase kinase kinase 2 (MAP4K2]. *J Med Chem*. 2015;58:183–196.
22. https://tools.thermofisher.com/content/sfs/manuals/MAP3K7_LanthaScreen_Binding.pdf.
23. Neumann E, Lefevre S, Zimmermann B, Gay S, Muller-Ladner U. Rheumatoid arthritis progression mediated by activated synovial fibroblasts. *Trends Mol Med*. 2010;16:458–468.
24. Jones DS, Jenney AP, Swantek JL, Burke JM, Lauffenburger DA, Sorger PK. Profiling drugs for rheumatoid arthritis that inhibit synovial fibroblast activation. *Nat Chem Biol*. 2016. http://dx.doi.org/10.1038/nchembio.2211.
25. Malemud CJ. Growth hormone, VEGF and FGF: involvement in rheumatoid arthritis. *Clin Chim Acta*. 2007;375:10–19.
26. Reddy AS, Zhang S. Polypharmacology: drug discovery for the future. *Expert Rev Clin Pharmacol*. 2013;6:41–47.
27. Slamon D, Eiermann W, Robert N, et al. Phase III randomized trial comparing doxorubicin and cyclophosphamide followed by docetaxel (AC → T) with doxorubicin and cyclophosphamide followed by docetaxel and trastuzumab

(AC → TH) with docetaxel, carboplatin and trastuzumab (TCH) in Her2neu positive early breast cancer patients: BCIRG 006 study. *Cancer Res*. 2009;69:62.
28. Canellos GP, Anderson JR, Propert KJ, et al. Chemotherapy of advanced Hodgkin's disease with MOPP, ABVD, or MOPP alternating with ABVD. *N Engl J Med*. 1992;327:1478–1484.
29. Albain KS, Rusch VW, Crowley JJ, et al. Concurrent cisplatin/etoposide plus chest radiotherapy followed by surgery for stages IIIA (N2) and IIIB non-small-cell lung cancer: mature results of Southwest Oncology Group phase II study 8805. *J Clin Oncol*. 1995;13:1880–1892.
30. Raney RB, Walterhouse DO, Meza JL, et al. Results of the Intergroup Rhabdomyosarcoma Study Group D9602 protocol, using vincristine and dactinomycin with or without cyclophosphamide and radiation therapy, for newly diagnosed patients with low-risk embryonal rhabdomyosarcoma: a report from the Soft Tissue Sarcoma Committee of the Children's Oncology Group. *J Clin Oncol*. 2011;29:1312–1318.
31. Webster RM. Combination therapies in oncology. *Nat Rev Drug Discovery*. 2016;15:81–82.
32. Peters JU. Polypharmacology – foe or friend? *J Med Chem*. 2013;56:8955–8971.
33. Llovet JM, Ricci S, Mazzaferro V, et al. Sorafenib in advanced hepatocellular carcinoma. *N Engl J Med*. 2008;359:378–390.
34. Adnane L, Trail PA, Taylor I, Wilhelm SM. Sorafenib (BAY 43-9006, Nexavar®), a dual-action inhibitor that targets RAF/MEK/ERK pathway in tumor cells and tyrosine kinases VEGFR/PDGFR in tumor vasculature. *Methods Enzymol*. 2006;407:597–612.
35. Cabanillas ME, Schlumberger M, Jarzab B, et al. A phase 2 trial of lenvatinib (E7080) in advanced, progressive, radioiodine-refractory, differentiated thyroid cancer: a clinical outcomes and biomarker assessment. *Cancer*. 2015;121:2749–2756.
36. Weisberg E, Nonami A, Chen Z, et al. Upregulation of IGF1R by mutant RAS in leukemia and potentiation of RAS signaling inhibitors by small-molecule inhibition of IGF1R. *Clin Cancer Res*. 2014;20:5483–5495.
37. Chen EY, Tan CM, Kou Y, et al. Enrichr: interactive and collaborative HTML5 gene list enrichment analysis tool. *BMC Bioinformatics*. 2013;14:128.
38. Kuleshov MV, Jones MR, Rouillard AD, et al. Enrichr: a comprehensive gene set enrichment analysis web server 2016 update. *Nucleic Acids Res*. 2016;44:W90–W97.
39. Oliveros JC (2007–2015) Venny. An interactive tool for comparing lists with Venn's diagrams, http://bioinfogp.cnb.csic.es/tools/venny/index.html.